

A Neural Tangent Kernel Formula for Ensembles of Soft Trees with Arbitrary Architectures

Ryuichi Kanoh^{1,2}, Mahito Sugiyama^{1,2}

¹National Institute of Informatics

²The Graduate University for Advanced Studies, SOKENDAI

{kanoh, mahito}@nii.ac.jp

Abstract

A *soft tree* is an actively studied variant of a decision tree that updates splitting rules using the gradient method. Although it can have various tree architectures, the theoretical properties of their impact are not well known. In this paper, we formulate and analyze the *Neural Tangent Kernel* (NTK) induced by *soft tree ensembles* for arbitrary tree architectures. This kernel leads to the remarkable finding that only the number of leaves at each depth is relevant for the tree architecture in ensemble learning with infinitely many trees. In other words, if the number of leaves at each depth is fixed, the training behavior in function space and the generalization performance are exactly the same across different tree architectures, even if they are not isomorphic. We also show that the NTK of asymmetric trees like decision lists does not degenerate when they get infinitely deep. This is in contrast to the perfect binary trees, whose NTK is known to degenerate and leads to worse generalization performance for deeper trees.

1 Introduction

Ensemble learning is one of the most important machine learning techniques used in real world applications. By combining the outputs of multiple predictors, one can obtain robust results for complex prediction problems. *Decision trees* are often used as weak learners in ensemble learning [1–3], and they can take a variety of structures such as various tree depths and whether or not the structure is symmetry. In the training process of tree ensembles, even a decision stump [4], a decision tree with a depth of 1, is known to be able to achieve zero training error as the number of trees increases [5]. Therefore, more complex weak learners are not required for training error minimization. However, generalization performance varies depending on weak learners [6], and theoretical properties of their impact are not well known, resulting in the requirement of empirical trial and error adjustments of the structure of weak learners.

We focus on a *soft tree* [7–9] as a weak learner in this paper. A soft tree is a variant of a decision tree that inherits characteristics of neural networks. Instead of using a greedy method [10, 11] to search splitting rules, soft trees make decision rules soft and simultaneously update the entire model parameters using the gradient method. Soft trees have been actively studied in recent years in terms of predictive performance [8, 12, 13], interpretability [9, 14], and potential techniques in real world applications like pre-training and fine-tuning [15, 16]. In addition, a soft tree can be interpreted as a particular case of Mixture-of-Experts [17–19], a practical technique for balancing computational cost and prediction performance.

To theoretically analyze the soft tree ensembles, Kanoh and Sugiyama [7] introduced the *Neural Tangent Kernel* (NTK) [20] induced by them. The NTK framework enables them to analytically describe the behavior of ensemble learning with infinitely many soft trees, which leads to several non-trivial properties such as global convergence of training and the effect of parameter sharing in an oblivious tree [12, 21]. However, their analysis is limited to perfect binary trees, and the

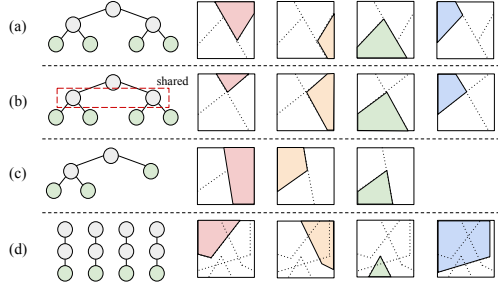


Figure 1: Schematic image of decision boundaries of the (a) perfect binary tree, (b) oblivious tree, (c) decision list, and (d) rule set.

theoretical properties of other tree architectures are still unrevealed. Figure 1 illustrates a variety of examples of tree architectures and their associated space partitioning in the case of a two-dimensional space. Note that each partition is not the axis parallel direction as we are considering soft trees. Not only symmetric trees, as shown in (a) and (b), but also asymmetric trees [22], as shown in (c), are often used in practical applications [23]. Moreover, the structure in (d) corresponds to the *rule set ensembles* [24], a combination of rules to obtain predictions, which can be viewed as a variant of trees. Although each of these architectures has a different space partitioning, it is not theoretically clear whether or not this makes any difference in the resulting predictive performance in ensemble learning.

In this paper, we study the NTK for soft trees with arbitrary architectures. We analytically derive the NTK that characterizes the training behavior of soft tree ensemble with arbitrary tree architectures and theoretically analyze the impact on generalization performance. Our contributions are summarized as follows:

- **The NTK for arbitrary trees is characterized by only the number of leaves per depth.**

We derive the NTK induced by an infinite rule set ensemble (Theorem 2). Using this kernel, we obtain a formula for the NTK induced by an infinite ensemble of trees with arbitrary architectures (Theorem 3), which generalizes [7, Theorem 1] about perfect binary trees. Interestingly, the kernel is determined by the number of leaves at each depth, which means that there are trees that induce the same NTK but are not isomorphic (Corollary 1).

- **The decision boundary sharing does not affect to the generalization performance.**

Since the kernel is determined by the number of leaves at each depth, for example, infinite ensembles with trees and rule sets shown in Figure 1(a) and (d) induce exactly the same NTKs. This means that the way of sharing decision boundaries does not change the model behavior within the limit of an infinite ensemble (Corollary 2).

- **The kernel degeneracy does not occur in deep asymmetric trees.**

The NTK induced by perfect binary trees degenerates when they get deeper: the kernel values become almost identical for deep trees even if the inner products between input pairs are different, resulting in poor performance in numerical experiments. In contrast, we find that the NTK does not degenerate for trees that grow in only one direction (Proposition 1); hence generalization performance does not become worse even if trees become infinitely deep (Proposition 2, Figure 8).

2 Preliminary

We introduce a formulation of soft trees, which we use as weak learners in ensemble learning, and review the basic properties of the NTK and the existing result for the perfect binary trees.

2.1 Soft Trees

We formulate regression by an ensemble of M soft trees. We define a data matrix $\mathbf{x} \in \mathbb{R}^{F \times N}$ composed of N training samples $\mathbf{x}_1, \dots, \mathbf{x}_N$ with F features. Each weak learner, indexed by

$m \in [M] = \{1, \dots, M\}$, has a parameter matrix $\mathbf{w}_m \in \mathbb{R}^{F \times \mathcal{N}}$ for internal nodes and $\boldsymbol{\pi}_m \in \mathbb{R}^{1 \times \mathcal{L}}$ for leaf nodes. They are in the following format:

$$\mathbf{x} = \left(\begin{array}{c|ccc|c} & & & & \\ \mathbf{x}_1 & \dots & \mathbf{x}_N & & \\ & & & & \\ \hline & & & & \\ \dots & & \dots & & \end{array} \right), \quad \mathbf{w}_m = \left(\begin{array}{c|ccc|c} & & & & \\ \mathbf{w}_{m,1} & \dots & \mathbf{w}_{m,\mathcal{N}} & & \\ & & & & \\ \hline & & & & \\ \dots & & \dots & & \end{array} \right), \quad \boldsymbol{\pi}_m = (\pi_{m,1}, \dots, \pi_{m,\mathcal{L}}),$$

where internal nodes and leaf nodes are indexed from 1 to \mathcal{N} and 1 to \mathcal{L} , respectively. For simplicity, we assume that \mathcal{N} and \mathcal{L} are the same across different weak learners throughout the paper. Horizontal concatenation of (column) vectors $\mathbf{x}_1, \dots, \mathbf{x}_N$ is denoted as $(\mathbf{x}_1, \dots, \mathbf{x}_N) = \mathbf{x} \in \mathbb{R}^{F \times \mathcal{N}}$ and $\mathbf{w}_{m,1}, \dots, \mathbf{w}_{m,\mathcal{N}}$ as $(\mathbf{w}_{m,1}, \dots, \mathbf{w}_{m,\mathcal{N}}) = \mathbf{w}_m \in \mathbb{R}^{F \times \mathcal{N}}$.

2.1.1 Internal nodes

In a soft tree, the splitting operation at an intermediate node $n \in [\mathcal{N}] = \{1, \dots, \mathcal{N}\}$ is not completely binary. To formulate the probabilistic splitting operation, we introduce the notation $\ell \swarrow n$ (resp. $n \searrow \ell$), which is a binary relation being true if a leaf $\ell \in [\mathcal{L}] = \{1, \dots, \mathcal{L}\}$ belongs to the left (resp. right) subtree of a node n and false otherwise. We also use an indicator function $\mathbb{1}_Q$ on the argument Q , i.e., $\mathbb{1}_Q = 1$ if Q is true and $\mathbb{1}_Q = 0$ otherwise. Every leaf node $\ell \in [\mathcal{L}]$ holds the probability that data reach to it, which is formulated as a function $\mu_{m,\ell} : \mathbb{R}^F \times \mathbb{R}^{F \times \mathcal{N}} \rightarrow [0, 1]$ defined as

$$\mu_{m,\ell}(\mathbf{x}_i, \mathbf{w}_m) = \prod_{n=1}^{\mathcal{N}} \underbrace{\sigma(\mathbf{w}_{m,n}^\top \mathbf{x}_i)}_{\text{flow to the left}}^{\mathbb{1}_{\ell \swarrow n}} \underbrace{(1 - \sigma(\mathbf{w}_{m,n}^\top \mathbf{x}_i))}_{\text{flow to the right}}^{\mathbb{1}_{n \searrow \ell}}, \quad (1)$$

where $\sigma : \mathbb{R} \rightarrow [0, 1]$ represents softened boolean operation at internal nodes. The obtained value $\mu_{m,\ell}(\mathbf{x}_i, \mathbf{w}_m)$ is the probability of a sample \mathbf{x}_i reaching a leaf ℓ in a soft tree m with its parameter matrix \mathbf{w}_m . If the output of a decision function σ takes only 0.0 or 1.0, this operation realizes the hard splitting used in typical decision trees. We do not explicitly use the bias term for simplicity as it can be technically treated as an additional feature.

Internal nodes perform a sigmoid-like decision function such as the scaled error function $\sigma(p) = \frac{1}{2} \operatorname{erf}(\alpha p) + \frac{1}{2} = \frac{1}{2} \left(\frac{2}{\sqrt{\pi}} \int_0^{\alpha p} e^{-t^2} dt \right) + \frac{1}{2}$, the two-class sparsemax $\sigma(p) = \operatorname{sparsemax}([\alpha p, 0])$ [25], or the two-class entmax $\sigma(p) = \operatorname{entmax}([\alpha p, 0])$ [26]. More precisely, any continuous function is possible if it is rotationally symmetric about the point $(0, 1/2)$ satisfying $\lim_{p \rightarrow \infty} \sigma(p) = 1$, $\lim_{p \rightarrow -\infty} \sigma(p) = 0$, and $\sigma(0) = 0.5$. Therefore theoretical results presented in this paper hold for a variety of sigmoid-like decision functions. When the scaling factor $\alpha \in \mathbb{R}^+$ [9] is infinitely large, sigmoid-like decision functions become step functions and represent the (hard) boolean operation.

Equation (1) applies to arbitrary binary tree architectures. Moreover, if the flow to the right node $(1 - \sigma(\mathbf{w}_{m,n}^\top \mathbf{x}_i))$ is replaced to be 0, it is clear that the resulting model corresponds to a *rule set* [24] and it can be represented as a linear graph. Note that the value $\sum_{\ell=1}^{\mathcal{L}} \mu_{m,\ell}(\mathbf{x}_i, \mathbf{w}_m)$ is always guaranteed to be 1 for any soft trees, while it is not guaranteed for rule sets.

2.1.2 Leaf nodes

The prediction for each \mathbf{x}_i from a weak learner m parameterized by \mathbf{w}_m and $\boldsymbol{\pi}_m$, represented as a function $f_m : \mathbb{R}^F \times \mathbb{R}^{F \times \mathcal{N}} \times \mathbb{R}^{1 \times \mathcal{L}} \rightarrow \mathbb{R}$, is given by

$$f_m(\mathbf{x}_i, \mathbf{w}_m, \boldsymbol{\pi}_m) = \sum_{\ell=1}^{\mathcal{L}} \pi_{m,\ell} \mu_{m,\ell}(\mathbf{x}_i, \mathbf{w}_m), \quad (2)$$

where $\pi_{m,\ell}$ denotes the response of a leaf ℓ of the weak learner m . This formulation means that the prediction output is the average of leaf values $\pi_{m,\ell}$ weighted by $\mu_{m,\ell}(\mathbf{x}_i, \mathbf{w}_m)$, the probability of assigning the sample \mathbf{x}_i to the leaf ℓ . In this model, \mathbf{w}_m and $\boldsymbol{\pi}_m$ are updated during training with a gradient method. If $\mu_{m,\ell}(\mathbf{x}_i, \mathbf{w}_m)$ takes only 1.0 for one leaf and 0.0 for the other leaves, the behavior of the soft tree is equivalent to a typical decision tree prediction.

2.1.3 Aggregation

When aggregating the output of multiple weak learners in ensemble learning, we divide the sum of the outputs by the square root of the number of weak learners, resulting in

$$f(\mathbf{x}_i, \mathbf{w}, \boldsymbol{\pi}) = \frac{1}{\sqrt{M}} \sum_{m=1}^M f_m(\mathbf{x}_i, \mathbf{w}_m, \boldsymbol{\pi}_m). \quad (3)$$

This $1/\sqrt{M}$ scaling is known to be essential in the existing NTK literature to use the weak law of the large numbers [20]. Each of model parameters $\mathbf{w}_{m,n}$ and $\boldsymbol{\pi}_{m,\ell}$ are initialized with zero-mean i.i.d. Gaussians with unit variances. We refer such an initialization as the *NTK initialization*.

2.2 Neural Tangent Kernel

We review the basic properties of the NTK and the NTK for perfect binary tree ensembles [7].

For any learning model function g , the NTK induced by g at a training time τ is formulated as a matrix $\widehat{\mathbf{H}}_\tau^* \in \mathbb{R}^{N \times N}$, in which each $(i, j) \in [N] \times [N]$ component is defined as

$$[\widehat{\mathbf{H}}_\tau^*]_{ij} := \widehat{\Theta}_\tau^*(\mathbf{x}_i, \mathbf{x}_j) := \left\langle \frac{\partial g(\mathbf{x}_i, \boldsymbol{\theta}_\tau)}{\partial \boldsymbol{\theta}_\tau}, \frac{\partial g(\mathbf{x}_j, \boldsymbol{\theta}_\tau)}{\partial \boldsymbol{\theta}_\tau} \right\rangle, \quad (4)$$

where $\widehat{\Theta}_\tau^* : \mathbb{R}^F \times \mathbb{R}^F \rightarrow \mathbb{R}$. The bracket $\langle \cdot, \cdot \rangle$ denotes the inner product and $\boldsymbol{\theta}_\tau \in \mathbb{R}^P$ is a concatenated vector of all the P trainable model parameters at τ . An asterisk “*” indicates that the model is arbitrary. The model function $g : \mathbb{R}^F \times \mathbb{R}^P \rightarrow \mathbb{R}$ used in Equation (4) is expected to be applicable to a variety of model architectures. If we use soft trees introduced in Section 2.1 as weak learners, the NTK is formulated as $\sum_{m=1}^M \sum_{n=1}^N \left\langle \frac{\partial f(\mathbf{x}_i, \mathbf{w}, \boldsymbol{\pi})}{\partial \mathbf{w}_{m,n}}, \frac{\partial f(\mathbf{x}_j, \mathbf{w}, \boldsymbol{\pi})}{\partial \mathbf{w}_{m,n}} \right\rangle + \sum_{m=1}^M \sum_{\ell=1}^L \left\langle \frac{\partial f(\mathbf{x}_i, \mathbf{w}, \boldsymbol{\pi})}{\partial \boldsymbol{\pi}_{m,\ell}}, \frac{\partial f(\mathbf{x}_j, \mathbf{w}, \boldsymbol{\pi})}{\partial \boldsymbol{\pi}_{m,\ell}} \right\rangle$.

Suppose the NTK does not change from its initial value during training. In that case, one can describe the behavior of functional gradient descent with an infinitesimal step size under the squared loss using kernel ridge-less regression with the NTK [20, 27], which leads to the theoretical understanding of the training behavior. The kernel does not change from its initial value when considering an infinite width neural network [20] or an infinite number of soft tree ensembles [7] under the NTK initialization. Models with the same *limiting NTK*, which is the NTK induced by a model with infinite width or infinitely many weak learners, have exactly equivalent training behavior in function space.

The NTK induced by a soft tree ensemble with infinitely many perfect binary trees, that is, the NTK when $M \rightarrow \infty$, is known to be obtained in closed-form at initialization:

Theorem 1 ([7]). *The NTK for an ensemble of soft perfect binary trees with tree depth D converges in probability to the following deterministic kernel as $M \rightarrow \infty$,*

$$\begin{aligned} \Theta^{(D, \text{PB})}(\mathbf{x}_i, \mathbf{x}_j) &:= \lim_{M \rightarrow \infty} \widehat{\Theta}_0^{(D, \text{PB})}(\mathbf{x}_i, \mathbf{x}_j) \\ &= \underbrace{2^D D \Sigma(\mathbf{x}_i, \mathbf{x}_j) (\mathcal{T}(\mathbf{x}_i, \mathbf{x}_j))^{D-1} \dot{\mathcal{T}}(\mathbf{x}_i, \mathbf{x}_j)}_{\text{contribution from inner nodes}} + \underbrace{(2\mathcal{T}(\mathbf{x}_i, \mathbf{x}_j))^D}_{\text{contribution from leaves}}, \end{aligned} \quad (5)$$

where $\Sigma(\mathbf{x}_i, \mathbf{x}_j) := \mathbf{x}_i^\top \mathbf{x}_j$, $\mathcal{T}(\mathbf{x}_i, \mathbf{x}_j) := \mathbb{E}[\sigma(\mathbf{u}^\top \mathbf{x}_i) \sigma(\mathbf{u}^\top \mathbf{x}_j)]$, and $\dot{\mathcal{T}}(\mathbf{x}_i, \mathbf{x}_j) := \mathbb{E}[\dot{\sigma}(\mathbf{u}^\top \mathbf{x}_i) \dot{\sigma}(\mathbf{u}^\top \mathbf{x}_j)]$. Moreover, when the decision function is the scaled error function, $\mathcal{T}(\mathbf{x}_i, \mathbf{x}_j)$ and $\dot{\mathcal{T}}(\mathbf{x}_i, \mathbf{x}_j)$ are analytically obtained in the closed-form as

$$\mathcal{T}(\mathbf{x}_i, \mathbf{x}_j) = \frac{1}{2\pi} \arcsin \left(\frac{\alpha^2 \Sigma(\mathbf{x}_i, \mathbf{x}_j)}{\sqrt{(\alpha^2 \Sigma(\mathbf{x}_i, \mathbf{x}_i) + 0.5)(\alpha^2 \Sigma(\mathbf{x}_j, \mathbf{x}_j) + 0.5)}} \right) + \frac{1}{4}, \quad (6)$$

$$\dot{\mathcal{T}}(\mathbf{x}_i, \mathbf{x}_j) = \frac{\alpha^2}{\pi} \frac{1}{\sqrt{(1 + 2\alpha^2 \Sigma(\mathbf{x}_i, \mathbf{x}_i))(1 + 2\alpha^2 \Sigma(\mathbf{x}_j, \mathbf{x}_j)) - 4\alpha^4 \Sigma(\mathbf{x}_i, \mathbf{x}_j)^2}}. \quad (7)$$

Here, “PB” stands for a “P”erfect “B”inary tree. The dot used in $\dot{\sigma}(\mathbf{u}^\top \mathbf{x}_i)$ means the first derivative, and $\mathbb{E}[\cdot]$ means the expectation. The scalar π in Equation (6) and Equation (7) is the circular constant, and \mathbf{u} corresponds to $\mathbf{w}_{m,n}$ at any internal nodes. We can derive the formula of the limiting kernel by treating the number of trees in a tree ensemble like the width of the neural network, although the neural network and the soft tree ensemble are apparently different models.

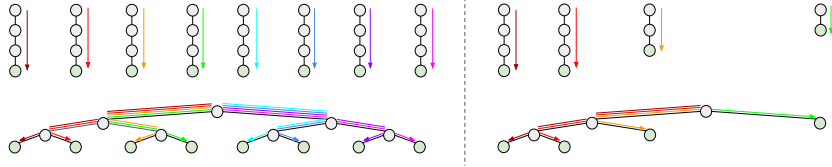


Figure 2: Correspondence between rule sets and binary trees. The top shows the corresponding rule sets for the bottom tree architectures.

3 Theoretical Results

We first consider rule set ensembles shown in Figure 1(d) and provide its NTK in Section 3.1. This becomes the key component to introduce the NTKs for trees with arbitrary architectures in Section 3.2. Due to space limitations, detailed proofs are given in the supplementary material.

3.1 NTK for Rule Sets

We prove that the NTK induced by a rule set ensemble is obtained in the closed-form as $M \rightarrow \infty$ at initialization:

Theorem 2. *The NTK for an ensemble of M soft rule sets with the depth D converges in probability to the following deterministic kernel as $M \rightarrow \infty$,*

$$\begin{aligned} \Theta^{(D, \text{Rule})}(\mathbf{x}_i, \mathbf{x}_j) &:= \lim_{M \rightarrow \infty} \widehat{\Theta}_0^{(D, \text{Rule})}(\mathbf{x}_i, \mathbf{x}_j) \\ &= \underbrace{D \Sigma(\mathbf{x}_i, \mathbf{x}_j) (\mathcal{T}(\mathbf{x}_i, \mathbf{x}_j))^{D-1} \dot{\mathcal{T}}(\mathbf{x}_i, \mathbf{x}_j)}_{\text{contribution from internal nodes}} + \underbrace{(\mathcal{T}(\mathbf{x}_i, \mathbf{x}_j))^D}_{\text{contribution from leaves}}, \end{aligned} \quad (8)$$

where $\Sigma(\mathbf{x}_i, \mathbf{x}_j)$, $\mathcal{T}(\mathbf{x}_i, \mathbf{x}_j)$ and $\dot{\mathcal{T}}(\mathbf{x}_i, \mathbf{x}_j)$ are the same with those in Theorem 1.

We can see that the limiting NTK induced by an infinite ensemble of 2^D rules coincides with the limiting NTK of the perfect binary tree in Theorem 1:

$$2^D \Theta^{(D, \text{Rule})}(\mathbf{x}_i, \mathbf{x}_j) = \Theta^{(D, \text{PB})}(\mathbf{x}_i, \mathbf{x}_j). \quad (9)$$

Here, 2^D corresponds to the number of leaves in a perfect binary tree. Figure 2 gives us an intuition: by duplicating internal nodes, we can always construct rule sets that correspond to a given tree by decomposing paths from the root to leaves, where the number of rules in the rule set corresponds to that of leaves in the tree.

3.2 NTK for Trees with Arbitrary Architectures

Using our interpretation that a tree is a combination of multiple rule sets, we can generalize Theorem 1 to include arbitrary tree architectures such as an asymmetric tree shown in the right panel of Figure 2.

Theorem 3. *Let $\mathcal{Q} : \mathbb{N} \rightarrow \mathbb{N} \cup \{0\}$ be a function that receives any depth and returns the number of leaves connected to internal nodes at the input depth. For any tree architecture, the NTK for an ensemble of soft trees converges in probability to the following deterministic kernel as $M \rightarrow \infty$,*

$$\Theta^{(\text{ArbitraryTree})}(\mathbf{x}_i, \mathbf{x}_j) := \lim_{M \rightarrow \infty} \widehat{\Theta}_0^{(\text{ArbitraryTree})}(\mathbf{x}_i, \mathbf{x}_j) = \sum_{d=1}^D \mathcal{Q}(d) \Theta^{(d, \text{Rule})}(\mathbf{x}_i, \mathbf{x}_j). \quad (10)$$

We can see that this formula covers the limiting NTK for perfect binary trees $2^D \Theta^{(D, \text{Rule})}(\mathbf{x}_i, \mathbf{x}_j)$, shown in Equation (9), as a special case by letting $\mathcal{Q}(D) = 2^D$ and 0 otherwise. Since this formula tells us that the limiting NTK only depends on the number of leaves at each depth with respect to tree architecture, the following holds:

Corollary 1. *The same limiting NTK can be induced from trees that are not isomorphic.*

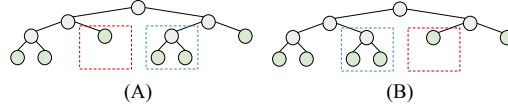


Figure 3: An example of non-isomorphic binary tree architectures that induce the same limiting NTK.

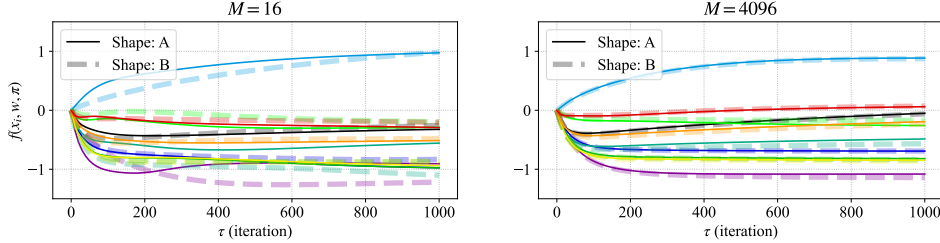


Figure 4: Output dynamics for test data points.

For example, for two trees illustrated in Figure 3, $\mathcal{Q}(1) = 0$, $\mathcal{Q}(2) = 2$, and $\mathcal{Q}(3) = 4$ for both left and right trees. Therefore, the limiting NTKs are identical for ensembles of these trees and become $2\Theta^{(2,\text{Rule})}(\mathbf{x}_i, \mathbf{x}_j) + 4\Theta^{(3,\text{Rule})}(\mathbf{x}_i, \mathbf{x}_j)$. Since they have the same limiting NTKs, their training behaviors in function space and generalization performances are exactly equivalent when we consider infinite ensembles, although they are not isomorphic and were expected to have different properties.

To empirically see this phenomenon, we have trained two types of ensembles; one is composed of soft trees in the left architecture in Figure 3 and the other is in the right architecture in Figure 3. We have tried two settings, $M = 16$ and $M = 4096$, to see the effect of the number of trees (weak learners). The decision function is a scaled error function with $\alpha = 2.0$. Figure 4 shows trajectories during full-batch gradient descent with a learning rate of 0.1. Initial outputs are shifted to zero [28]. There are 10 randomly generated training points and 10 randomly generated test data points, and their dimensionality $F = 5$. Each line corresponds to each data point, and solid and dotted lines denote ensembles of left and right architecture, respectively. This result shows that two trajectories (solid and dotted lines for each color) become similar if M is large, meaning that the property shown in Corollary 1 is empirically effective.

When we compare a rule set and a tree under the same number of leaves as shown in Figure 1(a) and (d), it is clear that the rule set has a larger representation power as it has more internal nodes and no decision boundaries are shared. However, when the collection of paths from the root to leaves in a tree is the same as the corresponding rule set as shown in Figure 2, their limiting NTKs are equivalent. Therefore, the following corollary holds:

Corollary 2. *Sharing decision boundaries by the parameter sharing does not affect to the limiting NTKs.*

Kanoh and Sugiyama [7] have shown that the kernel induced by the oblivious tree, as shown in Figure 1(b), converges to the same kernel induced by a non-oblivious one, as shown in Figure 1(a), in the limit of infinite trees. This corollary generalizes their result. This corollary implies that, when considering ensemble learning, a simple model like an oblivious tree can be a better choice if one uses a large number of weak learners as it is more efficient in terms of the number of parameters than the rule set ensemble.

4 Case Study: Decision List

As a typical example of asymmetric trees, we consider a tree that grows in only one direction, as shown in Figure 5, typically called a *decision list* [22] and commonly used in practical applications [29]. In this architecture, one leaf exists at each depth, except for leaves at the final depth where there are two.

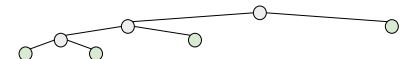


Figure 5: Decision list: a binary tree that grows in only one direction.

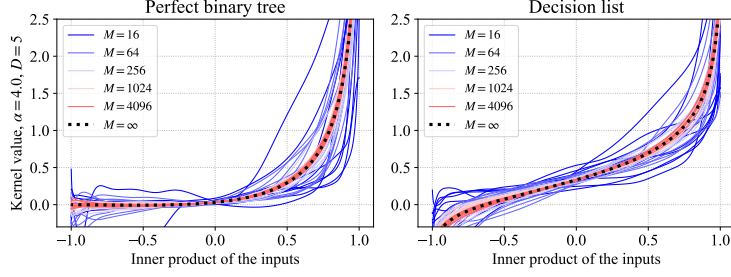


Figure 6: An empirical demonstration for (Left) perfect binary tree and (Right) decision list ensembles on the convergence of $\widehat{\Theta}_0^{(5,\text{PB})}(\mathbf{x}_i, \mathbf{x}_j)$ and $\widehat{\Theta}_0^{(5,\text{DL})}(\mathbf{x}_i, \mathbf{x}_j)$ to the fixed limit $\Theta^{(5,\text{PB})}(\mathbf{x}_i, \mathbf{x}_j)$ and $\Theta^{(5,\text{DL})}(\mathbf{x}_i, \mathbf{x}_j)$ as M increases.

4.1 NTK for Decision Lists

We show that the NTK induced by decision lists is formulated in closed-form as $M \rightarrow \infty$ at initialization:

Proposition 1. *The NTK for an ensemble of soft decision lists with the depth D converges in probability to the following deterministic kernel as $M \rightarrow \infty$,*

$$\begin{aligned}
\Theta^{(D,\text{DL})}(\mathbf{x}_i, \mathbf{x}_j) &:= \lim_{M \rightarrow \infty} \widehat{\Theta}_0^{(D,\text{DL})}(\mathbf{x}_i, \mathbf{x}_j) \\
&= \Theta^{(1,\text{Rule})}(\mathbf{x}_i, \mathbf{x}_j) + \Theta^{(2,\text{Rule})}(\mathbf{x}_i, \mathbf{x}_j) + \dots + 2\Theta^{(D,\text{Rule})}(\mathbf{x}_i, \mathbf{x}_j) \\
&= \Sigma(\mathbf{x}_i, \mathbf{x}_j) \dot{\mathcal{T}}(\mathbf{x}_i, \mathbf{x}_j) \underbrace{\left(\sum_{d=1}^D \left(d(\mathcal{T}(\mathbf{x}_i, \mathbf{x}_j))^{d-1} \right) + D(\mathcal{T}(\mathbf{x}_i, \mathbf{x}_j))^{D-1} \right)}_{\text{contribution from inner nodes}} \\
&\quad + \underbrace{\sum_{d=1}^D \left((\mathcal{T}(\mathbf{x}_i, \mathbf{x}_j))^d \right) + (\mathcal{T}(\mathbf{x}_i, \mathbf{x}_j))^D}_{\text{contribution from leaves}}, \tag{11}
\end{aligned}$$

where $\Sigma(\mathbf{x}_i, \mathbf{x}_j)$, $\mathcal{T}(\mathbf{x}_i, \mathbf{x}_j)$ and $\dot{\mathcal{T}}(\mathbf{x}_i, \mathbf{x}_j)$ are the same with those in Theorem 1.

In Proposition 1, ‘‘DL’’ stands for a ‘‘D’’ecision ‘‘L’’ist. The first equation comes from Theorem 3.

We numerically demonstrate the convergence of the kernels for perfect binary trees and decision lists in Figure 6 when the number M of trees gets larger. We use two simple inputs: $\mathbf{x}_i = \{1, 0\}$ and $\mathbf{x}_j = \{\cos(\beta), \sin(\beta)\}$ with $\beta = [0, \pi]$. The scaled error function is used as a decision function. The kernel induced by finite trees is numerically calculated 10 times with parameter re-initialization for each of $M = 16, 64, 256, 1024$, and 4096 . We empirically observe that the kernels induced by sufficiently many soft trees converge to the limiting kernel given in Equations (5) and (11) shown by the dotted lines in Figure 6. The kernel values induced by a finite ensemble are already close to the limiting NTK if the number of trees is larger than several hundred, which is a typical order of the number of trees in practical applications [12]. This indicates that our NTK analysis is also effective in practical applications with finite ensembles.

4.2 Degeneracy

Next, we analyze the effect of the tree depth to the kernel values. It is known that too deep soft perfect binary trees induce the *degeneracy* phenomenon [7], and we analyze whether or not this phenomenon also occurs in asymmetric trees like decision lists. Since $0 < \mathcal{T}(\mathbf{x}_i, \mathbf{x}_j) < 0.5$, replacing the summation in Equation (11) with an infinite series, we can obtain the closed-form formula when the depth $D \rightarrow \infty$ in the case of decision lists:

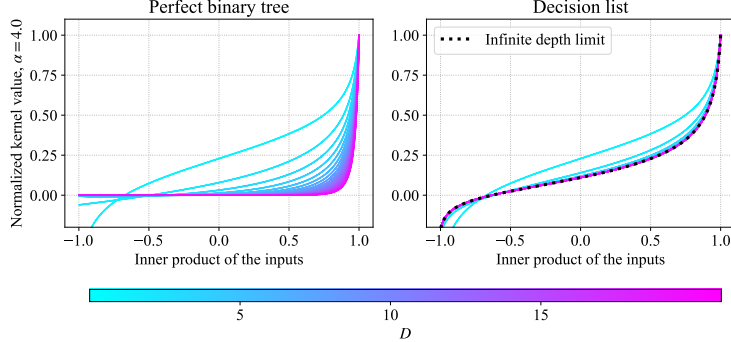


Figure 7: Depth dependency of (Left) $\Theta^{(D,\text{PB})}(\mathbf{x}_i, \mathbf{x}_j)$ and (Right) $\Theta^{(D,\text{DL})}(\mathbf{x}_i, \mathbf{x}_j)$. For decision lists, the limit of infinite depth is indicated by the dotted line.

Proposition 2. *The NTK for an ensemble of soft decision lists with an infinite depth converges in probability to the following deterministic kernel as $M \rightarrow \infty$,*

$$\lim_{D \rightarrow \infty} \Theta^{(D,\text{DL})}(\mathbf{x}_i, \mathbf{x}_j) = \underbrace{\frac{\Sigma(\mathbf{x}_i, \mathbf{x}_j) \dot{\mathcal{T}}(\mathbf{x}_i, \mathbf{x}_j)}{(1 - \mathcal{T}(\mathbf{x}_i, \mathbf{x}_j))^2}}_{\text{contribution from inner nodes}} + \underbrace{\frac{\mathcal{T}(\mathbf{x}_i, \mathbf{x}_j)}{1 - \mathcal{T}(\mathbf{x}_i, \mathbf{x}_j)}}_{\text{contribution from leaves}}, \quad (12)$$

where definitions of $\Sigma(\mathbf{x}_i, \mathbf{x}_j)$, $\mathcal{T}(\mathbf{x}_i, \mathbf{x}_j)$ and $\dot{\mathcal{T}}(\mathbf{x}_i, \mathbf{x}_j)$ are the same with those in Theorem 1.

Thus the limiting NTK $\Theta^{(D,\text{DL})}$ of decision lists neither degenerates nor diverges as $D \rightarrow \infty$.

Figure 7 shows how the kernel changes as depth changes. In the case of the perfect binary tree, the kernel value sticks to zero as the inner product of the input gets farther from 1.0 [7], whereas in the decision list case, the kernel value does not stick to zero. In other words, deep perfect binary trees cannot distinguish between vectors with a 90-degree difference in angle and vectors with a 180-degree difference in angle. Meanwhile, even if the decision list becomes infinitely deep, the kernel does not degenerate as shown by the dotted line in the right panel of Figure 7. It implies that a deterioration in generalization performance is not likely to occur even if the model gets infinitely deep. We can understand such behavior intuitively from the following reasoning. When the depth of the perfect binary tree is infinite, all splitting regions become infinitely small, hence every data point falls into a unique leaf. In contrast, when a decision list is used, large splitting regions remain, so not all data are separated. This can avoid the phenomenon of separating data being equally distant.

4.3 Numerical Experiments

We experimentally examine the effects of the degeneracy phenomenon discussed in Section 4.2.

Setup. We use 90 classification tasks in the UCI database [30], each of which has fewer than 5000 data points as in [31]. We performed kernel regression using the limiting NTK defined in Equations (5) and (11), equivalent to the infinite ensemble of the perfect binary trees and decision lists. We use D in $\{2, 4, 8, 16, 32, 64, 128\}$ and α in $\{1.0, 2.0, 4.0, 8.0, 16.0, 32.0\}$. The scaled error function is used as a decision function. To consider the ridge-less situation, regularization strength is fixed to 1.0×10^{-8} , a very small constant. We follow the procedures by Arora et al. [31] and Fernández-Delgado et al. [32]: We report 4-fold cross-validation performance with random data splitting. Other details are provided in the supplementary material.

Performance. Figure 8 shows the averaged performance in classification accuracy on 90 datasets. The generalization performance decreases as the tree depth increases when perfect binary trees are used as weak learners. However, no significant deterioration occurs when decision lists are used as weak learners. This result is consistent with the degeneracy properties as discussed in Section 4.2. The performance of decision lists already becomes almost consistent with their infinite depth limit when the depth reaches around 10. This suggests that we will no longer see significant changes in output for deeper decision lists. For small α , asymmetric trees often perform better than symmetric trees, but the characteristics reverse for large α .

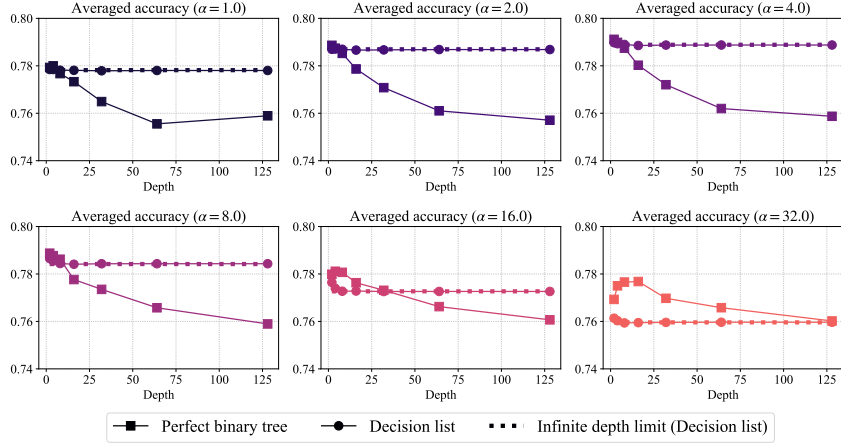


Figure 8: Averaged accuracy over 90 dataset. Horizontal dotted lines show the accuracy of decision lists with the infinite depth limit. The statistical significance is assessed in the supplementary material.

Computational Complexity of the Kernel. Let $U = \sum_{d=1}^D \mathbb{1}_{Q(d)>0}$, the number of depths connected to leaves. In general, the complexity for computing each kernel value for a pair of samples is $O(U)$. However, there are cases in which we can reduce the complexity to $O(1)$, for example, in the case of an infinitely deep decision list as shown in Proposition 2, although $U = \infty$.

5 Discussions

Application to Neural Architecture Search (NAS). Arora et al. [33] propose to use the NTK for *Neural Architecture Search* (NAS) [34] for performance estimation. Such studies have been active in recent years [35–37]. Our findings allow us to reduce the number of tree architecture candidates significantly. Theorem 3 tells us the existence of redundant architectures that do not need to be explored in NAS. Numerical experiments shown in Figure 8 suggest that we do not need to explore extremely deep tree structures even with asymmetric tree architecture.

Analogy between decision lists and residual networks. Huang et al. [38] show that although the multi-layer perceptron without skip-connection [39] exhibits the degeneracy phenomenon, the multi-layer perceptron with skip-connection does not exhibit it. This is common to our situation, where skip-connection for the multi-layer perceptron corresponds to asymmetric structure for soft trees like decision lists. Moreover, Veit et al. [40] propose an interpretation of residual networks showing that they can be seen as a collection of many paths of differing lengths. This is also similar to us because decision lists can be viewed as a collection of paths, i.e., rule sets, with different lengths. Therefore our findings in this paper suggest that there may be a common reason why performance does not deteriorate easily as the depth increases.

6 Conclusions

We have introduced and studied the NTK induced by arbitrary tree architectures. Our theoretical analysis via the kernel provides new insights into the behavior of the infinite ensemble of soft trees: for different soft trees, if the number of leaves per depth is equal, the training behavior of their infinite ensembles in function space matches exactly, even if the tree architectures are not isomorphic. Moreover, we have theoretically and empirically shown that the deepening of asymmetric trees like decision lists does not necessarily induce the degeneracy phenomenon, although it occurs in symmetric perfect binary trees.

Limitations and social impacts. NTK-based analyses have limitations. NTKs are analyzed only under a specific regime (e.g., lazy training [28]). Therefore, there still exists a theoretical gap between NTKs and practical models [33]. We will leave these challenges for future investigation. This study is a theoretical analysis of ensemble learning, and we believe that our theoretical discussion will not have negative societal impacts.

References

- [1] Leo Breiman. Random Forests. In *Machine Learning*, 2001.
- [2] Tianqi Chen and Carlos Guestrin. XGBoost: A scalable tree boosting system. In *Proceedings of the 22nd ACM SIGKDD International Conference on Knowledge Discovery and Data Mining*, 2016.
- [3] Guolin Ke, Qi Meng, Thomas Finley, Taifeng Wang, Wei Chen, Weidong Ma, Qiwei Ye, and Tie-Yan Liu. LightGBM: A Highly Efficient Gradient Boosting Decision Tree. In *Advances in Neural Information Processing Systems*, 2017.
- [4] Wayne Iba and Pat Langley. Induction of One-Level Decision Trees. In *Machine Learning Proceedings*. Morgan Kaufmann, 1992.
- [5] Yoav Freund and Robert E. Schapire. Experiments with a New Boosting Algorithm. In *Proceedings of the Thirteenth International Conference on International Conference on Machine Learning*, 1996.
- [6] C. H. Bryan Liu, Benjamin Paul Chamberlain, Duncan A. Little, and Ângelo Cardoso. Generalising Random Forest Parameter Optimisation to Include Stability and Cost. In *Machine Learning and Knowledge Discovery in Databases*, 2017.
- [7] Ryuichi Kanoh and Mahito Sugiyama. A Neural Tangent Kernel Perspective of Infinite Tree Ensembles. In *International Conference on Learning Representations*, 2022.
- [8] Peter Kortschieder, Madalina Fiterau, Antonio Criminisi, and Samuel Rota Bulò. Deep Neural Decision Forests. In *IEEE International Conference on Computer Vision*, 2015.
- [9] Nicholas Frosst and Geoffrey E. Hinton. Distilling a Neural Network Into a Soft Decision Tree. *CoRR*, 2017.
- [10] J. R. Quinlan. Induction of Decision Trees. *Machine Learning*, 1986.
- [11] Leo Breiman, Jerome Friedman, Charles J. Stone, and R.A. Olshen. *Classification and Regression Trees*. Chapman and Hall/CRC, 1984.
- [12] Sergei Popov, Stanislav Morozov, and Artem Babenko. Neural Oblivious Decision Ensembles for Deep Learning on Tabular Data. In *International Conference on Learning Representations*, 2020.
- [13] Hussein Hazimeh, Natalia Ponomareva, Petros Mol, Zhenyu Tan, and Rahul Mazumder. The Tree Ensemble Layer: Differentiability meets Conditional Computation. In *Proceedings of the 37th International Conference on Machine Learning*, 2020.
- [14] Alvin Wan, Lisa Dunlap, Daniel Ho, Jihan Yin, Scott Lee, Suzanne Petryk, Sarah Adel Bargal, and Joseph E. Gonzalez. NBDT: Neural-Backed Decision Tree. In *International Conference on Learning Representations*, 2021.
- [15] Guolin Ke, Zhenhui Xu, Jia Zhang, Jiang Bian, and Tie-Yan Liu. DeepGBM: A Deep Learning Framework Distilled by GBDT for Online Prediction Tasks. In *Proceedings of the 25th ACM SIGKDD International Conference on Knowledge Discovery & Data Mining*, 2019.
- [16] Sercan Ömer Arik and Tomas Pfister. TabNet: Attentive Interpretable Tabular Learning. *CoRR*, 2019.
- [17] M.I. Jordan and R.A. Jacobs. Hierarchical mixtures of experts and the EM algorithm. In *Proceedings of International Conference on Neural Networks*, 1993.
- [18] Noam Shazeer, Azalia Mirhoseini, Krzysztof Maziarz, Andy Davis, Quoc V. Le, Geoffrey E. Hinton, and Jeff Dean. Outrageously Large Neural Networks: The Sparsely-Gated Mixture-of-Experts Layer. In *International Conference on Learning Representations*, 2017.

[19] Dmitry Lepikhin, HyoukJoong Lee, Yuanzhong Xu, Dehao Chen, Orhan Firat, Yanping Huang, Maxim Krikun, Noam Shazeer, and Zhifeng Chen. GShard: Scaling Giant Models with Conditional Computation and Automatic Sharding. In *International Conference on Learning Representations*, 2021.

[20] Arthur Jacot, Franck Gabriel, and Clement Hongler. Neural Tangent Kernel: Convergence and Generalization in Neural Networks. In *Advances in Neural Information Processing Systems*, 2018.

[21] Liudmila Prokhorenkova, Gleb Gusev, Aleksandr Vorobev, Anna Veronika Dorogush, and Andrey Gulin. CatBoost: unbiased boosting with categorical features. In *Advances in Neural Information Processing Systems*, 2018.

[22] Ronald L. Rivest. Learning Decision Lists. *Machine Language.*, 1987.

[23] Ryutaro Tanno, Kai Arulkumaran, Daniel Alexander, Antonio Criminisi, and Aditya Nori. Adaptive Neural Trees. In *Proceedings of the 36th International Conference on Machine Learning*, 2019.

[24] Jerome H. Friedman and Bogdan E. Popescu. Predictive learning via rule ensembles. *The Annals of Applied Statistics*, 2008.

[25] Andre Martins and Ramon Astudillo. From Softmax to Sparsemax: A Sparse Model of Attention and Multi-Label Classification. In *Proceedings of The 33rd International Conference on Machine Learning*, 2016.

[26] Ben Peters, Vlad Niculae, and André F. T. Martins. Sparse Sequence-to-Sequence Models. In *Proceedings of the 57th Annual Meeting of the Association for Computational Linguistics*, 2019.

[27] Jaehoon Lee, Lechao Xiao, Samuel Schoenholz, Yasaman Bahri, Roman Novak, Jascha Sohl-Dickstein, and Jeffrey Pennington. Wide Neural Networks of Any Depth Evolve as Linear Models Under Gradient Descent. In *Advances in Neural Information Processing Systems*, 2019.

[28] Lénaïc Chizat, Edouard Oyallon, and Francis Bach. On Lazy Training in Differentiable Programming. In *Advances in Neural Information Processing Systems*, 2019.

[29] Benjamin Letham, Cynthia Rudin, Tyler H. McCormick, and David Madigan. Interpretable classifiers using rules and Bayesian analysis: Building a better stroke prediction model. *The Annals of Applied Statistics*, 2015.

[30] Dheeru Dua and Casey Graff. UCI Machine Learning Repository, 2017.

[31] Sanjeev Arora, Simon S. Du, Zhiyuan Li, Ruslan Salakhutdinov, Ruosong Wang, and Dingli Yu. Harnessing the Power of Infinitely Wide Deep Nets on Small-data Tasks. In *International Conference on Learning Representations*, 2020.

[32] Manuel Fernández-Delgado, Eva Cernadas, Senén Barro, and Dinani Amorim. Do we Need Hundreds of Classifiers to Solve Real World Classification Problems? *Journal of Machine Learning Research*, 2014.

[33] Sanjeev Arora, Simon S Du, Wei Hu, Zhiyuan Li, Russ R Salakhutdinov, and Ruosong Wang. On Exact Computation with an Infinitely Wide Neural Net. In *Advances in Neural Information Processing Systems*, 2019.

[34] Thomas Elsken, Jan Hendrik Metzen, and Frank Hutter. Neural Architecture Search: A Survey. *Journal of Machine Learning Research*, 2019.

[35] Wuyang Chen, Xinyu Gong, and Zhangyang Wang. Neural Architecture Search on ImageNet in Four GPU Hours: A Theoretically Inspired Perspective. In *International Conference on Learning Representations*, 2021.

[36] Jingjing Xu, Liang Zhao, Junyang Lin, Rundong Gao, Xu Sun, and Hongxia Yang. KNAS: Green Neural Architecture Search. In *Proceedings of the 38th International Conference on Machine Learning*, 2021.

- [37] Jisoo Mok, Byunggoon Na, Ji-Hoon Kim, Dongyoong Han, and Sungroh Yoon. Demystifying the Neural Tangent Kernel from a Practical Perspective: Can it be trusted for Neural Architecture Search without training? In *IEEE Conference on Computer Vision and Pattern Recognition*, 2022.
- [38] Kaixuan Huang, Yuqing Wang, Molei Tao, and Tuo Zhao. Why Do Deep Residual Networks Generalize Better than Deep Feedforward Networks? — A Neural Tangent Kernel Perspective. In *Advances in Neural Information Processing Systems*, 2020.
- [39] Kaiming He, Xiangyu Zhang, Shaoqing Ren, and Jian Sun. Deep Residual Learning for Image Recognition. In *IEEE Conference on Computer Vision and Pattern Recognition*, 2016.
- [40] Andreas Veit, Michael J Wilber, and Serge Belongie. Residual Networks Behave Like Ensembles of Relatively Shallow Networks. In *Advances in Neural Information Processing Systems*, 2016.

A Proof of Theorem 2

Theorem 2. *The NTK for an ensemble of M soft rule sets with the depth D converges in probability to the following deterministic kernel as $M \rightarrow \infty$,*

$$\begin{aligned} \Theta^{(D, \text{Rule})}(\mathbf{x}_i, \mathbf{x}_j) &:= \lim_{M \rightarrow \infty} \widehat{\Theta}_0^{(D, \text{Rule})}(\mathbf{x}_i, \mathbf{x}_j) \\ &= \underbrace{D \Sigma(\mathbf{x}_i, \mathbf{x}_j) (\mathcal{T}(\mathbf{x}_i, \mathbf{x}_j))^{D-1} \dot{\mathcal{T}}(\mathbf{x}_i, \mathbf{x}_j)}_{\text{contribution from internal nodes}} + \underbrace{(\mathcal{T}(\mathbf{x}_i, \mathbf{x}_j))^D}_{\text{contribution from leaves}}, \end{aligned}$$

where $\Sigma(\mathbf{x}_i, \mathbf{x}_j)$, $\mathcal{T}(\mathbf{x}_i, \mathbf{x}_j)$ and $\dot{\mathcal{T}}(\mathbf{x}_i, \mathbf{x}_j)$ are the same with those in Theorem 1.

Proof. We consider the contribution from internal nodes $\Theta^{(D, \text{Rule, nodes})}$ and the contribution from leaves $\Theta^{(D, \text{Rule, leaves})}$ separately, such that

$$\Theta^{(D, \text{Rule})}(\mathbf{x}_i, \mathbf{x}_j) = \Theta^{(D, \text{Rule, nodes})}(\mathbf{x}_i, \mathbf{x}_j) + \Theta^{(D, \text{Rule, leaves})}(\mathbf{x}_i, \mathbf{x}_j). \quad (\text{A.1})$$

As for internal nodes, we have

$$\frac{f^{(D, \text{Rule})}(\mathbf{x}_i, \mathbf{w}, \boldsymbol{\pi})}{\partial \mathbf{w}_{m,t}} = \frac{1}{\sqrt{M}} \mathbf{x}_i \dot{\sigma}(\mathbf{w}_{m,t}^\top \mathbf{x}_i) f_m^{(D-1, \text{Rule})}(\mathbf{x}_i, \mathbf{w}_{m,-t}, \boldsymbol{\pi}_m), \quad (\text{A.2})$$

where we consider the derivative with respect to a node t , and $\mathbf{w}_{m,-t}$ denotes the internal node parameter matrix except for the parameters of the node t . Since there are D possible locations for t , we obtain

$$\Theta^{(D, \text{Rule, nodes})}(\mathbf{x}_i, \mathbf{x}_j) = D \Sigma(\mathbf{x}_i, \mathbf{x}_j) (\mathcal{T}(\mathbf{x}_i, \mathbf{x}_j))^{D-1} \dot{\mathcal{T}}(\mathbf{x}_i, \mathbf{x}_j), \quad (\text{A.3})$$

where

$$\begin{aligned} &\mathbb{E}_m \left[f_m^{(D, \text{Rule})}(\mathbf{x}_i, \mathbf{w}_m, \boldsymbol{\pi}_m) f_m^{(D, \text{Rule})}(\mathbf{x}_j, \mathbf{w}_m, \boldsymbol{\pi}_m) \right] \\ &= \mathbb{E}_m \left[\underbrace{\sigma(\mathbf{w}_{m,1}^\top \mathbf{x}_i) \sigma(\mathbf{w}_{m,1}^\top \mathbf{x}_j)}_{\rightarrow \mathcal{T}(\mathbf{x}_i, \mathbf{x}_j)} \underbrace{\sigma(\mathbf{w}_{m,2}^\top \mathbf{x}_i) \sigma(\mathbf{w}_{m,2}^\top \mathbf{x}_j)}_{\rightarrow \mathcal{T}(\mathbf{x}_i, \mathbf{x}_j)} \cdots \underbrace{\sigma(\mathbf{w}_{m,D}^\top \mathbf{x}_i) \sigma(\mathbf{w}_{m,D}^\top \mathbf{x}_j)}_{\rightarrow \mathcal{T}(\mathbf{x}_i, \mathbf{x}_j)} \underbrace{\pi_{m,1}^2}_{\rightarrow 1} \right] \\ &= (\mathcal{T}(\mathbf{x}_i, \mathbf{x}_j))^D \end{aligned} \quad (\text{A.4})$$

is used. Here, the subscription “ \rightarrow ” means that the expected value of the corresponding term will be.

Similarly, for leaves,

$$\frac{f^{(D, \text{Rule})}(\mathbf{x}_i, \mathbf{w}, \boldsymbol{\pi})}{\partial \pi_{m,1}} = \frac{1}{\pi_{m,1} \sqrt{M}} f_m^{(D, \text{Rule})}(\mathbf{x}_i, \mathbf{w}_m, \boldsymbol{\pi}_m), \quad (\text{A.5})$$

resulting in

$$\Theta^{(D, \text{Rule, leaves})}(\mathbf{x}_i, \mathbf{x}_j) = (\mathcal{T}(\mathbf{x}_i, \mathbf{x}_j))^D. \quad (\text{A.6})$$

Combining Equation (A.3) and (A.6), we obtain Equation (8). \square

B Proof of Theorem 3

Theorem 3. Let $\mathcal{Q} : \mathbb{N} \rightarrow \mathbb{N} \cup \{0\}$ be a function that receives any depth and returns the number of leaves connected to internal nodes at the input depth. For any tree architecture, the NTK for an ensemble of soft trees converges in probability to the following deterministic kernel as $M \rightarrow \infty$,

$$\Theta^{(\text{ArbitraryTree})}(\mathbf{x}_i, \mathbf{x}_j) := \lim_{M \rightarrow \infty} \widehat{\Theta}_0^{(\text{ArbitraryTree})}(\mathbf{x}_i, \mathbf{x}_j) = \sum_{d=1}^D \mathcal{Q}(d) \Theta^{(d, \text{Rule})}(\mathbf{x}_i, \mathbf{x}_j).$$

Proof. We separate leaf and inner node contributions.

Contribution from Inner Nodes. For a soft boolean operation, the following equations hold:

$$\begin{aligned} \mathbb{E}_m \left[(1 - \sigma(\mathbf{w}_{m,n}^\top \mathbf{x}_i)) (1 - \sigma(\mathbf{w}_{m,n}^\top \mathbf{x}_j)) \right] &= \mathbb{E}_m \left[1 - \underbrace{\sigma(\mathbf{w}_{m,n}^\top \mathbf{x}_i)}_{\rightarrow 0.5} - \underbrace{\sigma(\mathbf{w}_{m,n}^\top \mathbf{x}_j)}_{\rightarrow 0.5} \right. \\ &\quad \left. + \sigma(\mathbf{w}_{m,n}^\top \mathbf{x}_i) \sigma(\mathbf{w}_{m,n}^\top \mathbf{x}_j) \right] \\ &= \mathbb{E}_m [\sigma(\mathbf{w}_{m,n}^\top \mathbf{x}_i) \sigma(\mathbf{w}_{m,n}^\top \mathbf{x}_j)], \end{aligned} \quad (\text{B.1})$$

$$\begin{aligned} \mathbb{E}_m \left[\frac{\partial (1 - \sigma(\mathbf{w}_{m,n}^\top \mathbf{x}_i))}{\partial \mathbf{w}_{m,n}} \frac{\partial (1 - \sigma(\mathbf{w}_{m,n}^\top \mathbf{x}_j))}{\partial \mathbf{w}_{m,n}} \right] &= \mathbb{E}_m [\mathbf{x}_i^\top \mathbf{x}_j \dot{\sigma}(\mathbf{w}_{m,n}^\top \mathbf{x}_i) \dot{\sigma}(\mathbf{w}_{m,n}^\top \mathbf{x}_j)] \\ &= \mathbb{E}_m \left[\frac{\partial \sigma(\mathbf{w}_{m,n}^\top \mathbf{x}_i)}{\partial \mathbf{w}_{m,n}} \frac{\partial \sigma(\mathbf{w}_{m,n}^\top \mathbf{x}_j)}{\partial \mathbf{w}_{m,n}} \right]. \end{aligned} \quad (\text{B.2})$$

Since each $\sigma(\mathbf{w}_{m,n}^\top \mathbf{x}_i)$ becomes 0.5, although the term $1 - \sigma(\mathbf{w}_{m,n}^\top \mathbf{x}_i)$ is used instead of $\sigma(\mathbf{w}_{m,n}^\top \mathbf{x}_i)$ for the rightward flow in the tree, exactly the same limiting NTK can be obtained by treating $1 - \sigma(\mathbf{w}_{m,n}^\top \mathbf{x}_i)$ as $\sigma(\mathbf{w}_{m,n}^\top \mathbf{x}_i)$.

As for an inner node contribution, the derivative is obtained as

$$\begin{aligned} \frac{\partial f^{(\text{ArbitraryTree})}(\mathbf{x}_i, \mathbf{w}, \boldsymbol{\pi})}{\partial \mathbf{w}_{m,n}} &= \frac{1}{\sqrt{M}} \sum_{\ell=1}^L \pi_{m,\ell} \frac{\partial \mu_{m,\ell}(\mathbf{x}_i, \mathbf{w}_m)}{\partial \mathbf{w}_{m,n}} \\ &= \frac{1}{\sqrt{M}} \sum_{\ell=1}^L \pi_{m,\ell} S_{n,\ell}(\mathbf{x}_i, \mathbf{w}_m) \mathbf{x}_i \dot{\sigma}(\mathbf{w}_{m,n}^\top \mathbf{x}_i), \end{aligned} \quad (\text{B.3})$$

where

$$S_{n,\ell}(\mathbf{x}, \mathbf{w}_m) := \left(\prod_{n'=1}^N \sigma(\mathbf{w}_{m,n'}^\top \mathbf{x}_i)^{\mathbb{1}_{(\ell \prec n') \& (n \neq n')}} (1 - \sigma(\mathbf{w}_{m,n'}^\top \mathbf{x}_i))^{\mathbb{1}_{(n' \succ \ell) \& (n \neq n')}} \right) (-1)^{\mathbb{1}_{n \succ \ell}}, \quad (\text{B.4})$$

and $\&$ is a logical conjunction. Since $\pi_{m,\ell}$ is initialized as zero-mean i.i.d. Gaussians with unit variances,

$$\mathbb{E}_m [\pi_{m,\ell} \pi_{m,\ell'}] = 0 \text{ if } \ell \neq \ell'. \quad (\text{B.5})$$

Therefore, the inner node contribution for the limiting NTK is

$$\begin{aligned} \Theta^{(\text{ArbitraryTree, nodes})}(\mathbf{x}_i, \mathbf{x}_j) &= \mathbb{E}_m \left[\sum_{\ell=1}^L \pi_{m,\ell}^2 S_{n,\ell}(\mathbf{x}_i, \mathbf{w}_m) S_{n,\ell}(\mathbf{x}_j, \mathbf{w}_m) \mathbf{x}_i^\top \mathbf{x}_j \dot{\sigma}(\mathbf{w}_{m,n}^\top \mathbf{x}_i) \dot{\sigma}(\mathbf{w}_{m,n}^\top \mathbf{x}_j) \right] \\ &= \Sigma(\mathbf{x}_i, \mathbf{x}_j) \dot{\mathcal{T}}(\mathbf{x}_i, \mathbf{x}_j) \mathbb{E}_m \left[\sum_{\ell=1}^L S_{n,\ell}(\mathbf{x}_i, \mathbf{w}_m) S_{n,\ell}(\mathbf{x}_j, \mathbf{w}_m) \right]. \end{aligned} \quad (\text{B.6})$$

Suppose leaf ℓ is connected to an internal node of depth d . With Equation (B.1) and (B.2), we obtain

$$\mathbb{E}_m [S_{n,\ell}(\mathbf{x}_i, \mathbf{w}_m) S_{n,\ell}(\mathbf{x}_j, \mathbf{w}_m)] = (\mathcal{T}(\mathbf{x}_i, \mathbf{x}_j))^{d-1}. \quad (\text{B.7})$$

Therefore, considering all leaves,

$$\Theta^{(\text{ArbitraryTree, nodes})}(\mathbf{x}_i, \mathbf{x}_j) = \sum_{d=1}^D \mathcal{Q}(d) \Theta^{(d, \text{Rule, nodes})}, \quad (\text{B.8})$$

where $\Theta^{(d, \text{Rule, nodes})}$ is introduced in Equation (A.3)

Contribution from Leaves. As for the contribution from leaves, the derivative is obtained as

$$\frac{\partial f^{(\text{ArbitraryTree})}(\mathbf{x}_i, \mathbf{w}, \boldsymbol{\pi})}{\partial \pi_{m,\ell}} = \frac{1}{\sqrt{M}} \mu_{m,\ell}(\mathbf{x}_i, \mathbf{w}_m). \quad (\text{B.9})$$

Since $\mathbf{w}_{m,n}$ used in $\mu_{m,\ell}(\mathbf{x}_i, \mathbf{w}_m)$ is initialized as zero-mean i.i.d. Gaussians, contribution from leaves on the limiting NTK induced by arbitrary tree architecture is:

$$\begin{aligned} \Theta^{(\text{ArbitraryTree, leaves})}(\mathbf{x}_i, \mathbf{x}_j) &= \mathbb{E}_m \left[\sum_{\ell=1}^{\mathcal{L}} \mu_{m,\ell}(\mathbf{x}_i, \mathbf{w}_m) \mu_{m,\ell}(\mathbf{x}_j, \mathbf{w}_m) \right] \\ &= \sum_{d=1}^D \mathcal{Q}(d) \Theta^{(d, \text{Rule, leaves})}, \end{aligned} \quad (\text{B.10})$$

where $\Theta^{(d, \text{Rule, leaves})}$ is introduced in Equation (A.6) □

C Details of Numerical Experiments

C.1 Dataset acquisition

We used the UCI datasets [30] preprocessed by Fernández-Delgado et al. [32], which are publicly available at <http://persoal.citius.usc.es/manuel.fernandez.delgado/papers/jmlr/data.tar.gz>. Since the size of the kernel is the square of the dataset size and too many data make training impractical, we used preprocessed UCI dataset with the number of samples smaller than 5000. Arora et al. [31] reported the bug in the preprocess when the explicit training/test split is given. Therefore, we did not use that dataset with explicit training/test split. As a consequence, 90 different dataset are available.

C.2 Model specifications

We used kernel regression implemented in scikit-learn¹. To perform ridge-less situation, the regularization strength is set to be 1.0×10^{-8} , a very small constant.

C.3 Computational resource

We used Ubuntu Linux (version: 4.15.0-117-generic) and ran all experiments on 2.20 GHz Intel Xeon E5-2698 CPU and 252 GB of memory.

C.4 Statistical significance

A Wilcoxon signed rank test is conducted for 90 datasets to check the statistical significance of the differences between performances on a perfect binary tree and a decision list. Figure A.1 shows the p-values. Statistically significant differences can be observed for areas where the differences appear large in Figure 8, such as when α is small and D is large. We use Bonferroni correction to account for multiple testing, and the resulting significance level of the p-value is about 0.0012 for 5 percent confidence level. An asterisk “*” is placed in Figure A.1 with statistically significant result even after

¹https://scikit-learn.org/stable/modules/generated/sklearn.kernel_ridge.KernelRidge.html

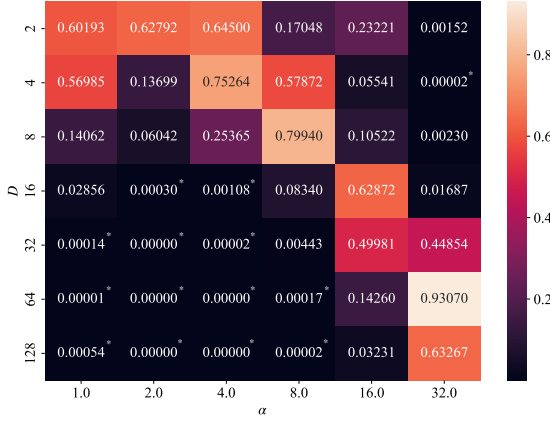


Figure A.1: P-values of the Wilcoxon signed rank test for results on perfect binary trees and decision lists with different parameters.

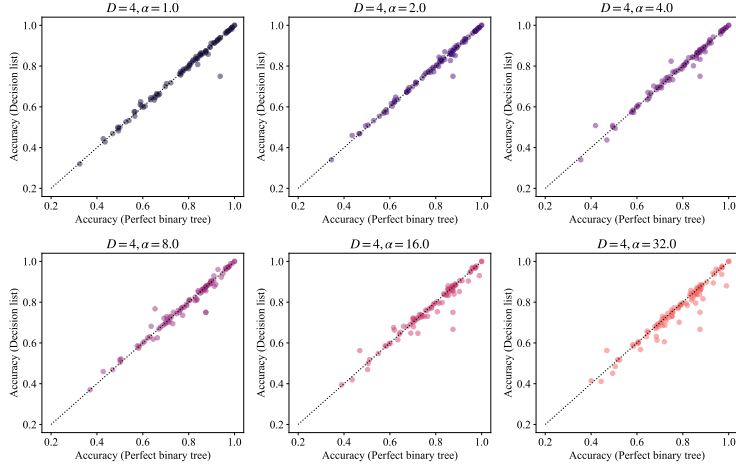


Figure A.2: Performance comparisons between the kernel regression with the limiting NTK induced by the perfect binary tree and the decision list on the UCI datasets with $D = 4$.

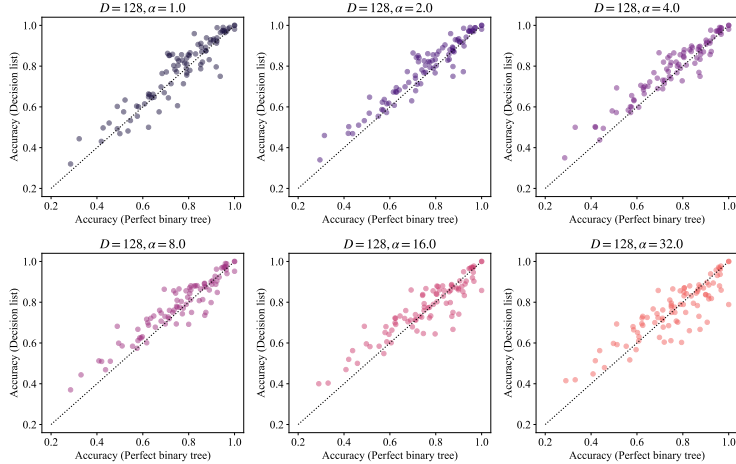


Figure A.3: Performance comparisons between the kernel regression with the limiting NTK induced by the perfect binary tree and the decision list on the UCI datasets with $D = 128$.

correction. For cases where the symmetry of the tree does not produce a large difference, such as at the depth of 2, the difference in performance is often not statistically significant.

Scatter-plots between the performance of the kernel regression with the limiting NTK induced by the perfect binary tree and the decision list are shown in Figures A.2 and A.3. The deeper the tree is, the larger the difference between them is.